

Antenna Health-Aware Selective Beamforming for Hardware-Constrained DFRC Systems II

Anis Hamadouche, Tharm Ratnarajah, Christos Masouros, John Thompson, and Mathini Sellathurai

Abstract—This study introduces an innovative beamforming design approach that incorporates the reliability of antenna array elements into the optimization process, termed "antenna health-aware selective beamforming". This method strategically focuses transmission power on more reliable antenna elements, thus enhancing system resilience and operational integrity. By integrating antenna health information and individual power constraints, our research leverages advanced optimization techniques such as the Group Proximal-Gradient Dual Ascent (GPGDA) to efficiently address nonconvex challenges in sparse array selection. Applying the proposed technique to a Dual-Functional Radar-Communication (DFRC) system, our findings highlight that increasing the sparsity promotion weight (ρ_s) generally boosts spectral efficiency and communication data rate, achieving perfect system reliability at higher ρ_s values but also revealing a performance threshold beyond which further sparsity is detrimental. This underscores the importance of balanced sparsity in beamforming for optimizing performance, particularly in critical communication and defense applications where uninterrupted operation is crucial. Additionally, our analysis of the time complexity and power consumption associated with GPGDA underscores the need for optimizing computational resources in practical implementations.

Index Terms—Dual Function Radar Communication (DFRC); Joint Radar-Communication (JRC); Beamforming; 5G; Optimization Algorithms.

I. INTRODUCTION

In today's cellular network landscape, the escalating demand for rapid and dependable communication has led to the evolution of more dynamic and adaptable system architectures. Contemporary cellular networks have transformed from static structures into active ecosystems that must continuously adjust to varying user needs, network conditions, and strict quality of service (QoS) standards. This flexibility is particularly crucial in Dual Function Radar Communication (DFRC) systems, where blending radar and communication within the same spectral space introduces distinct challenges and opportunities [9, 21, 6, 16, 4].

The adaptability of modern cellular networks is essential for several reasons. First, user demands are no longer homogenous or predictable but are varied and dynamic [1, 7, 5, 3, 2]. Users anticipate uninterrupted connectivity for activities ranging from streaming high-definition videos and

online gaming to using IoT devices in smart homes. Networks must dynamically allocate resources to meet these diverse needs without sacrificing speed, latency, or reliability [2].

Moreover, the operating environment for cellular networks is inherently dynamic. Elements such as user mobility, interference from adjacent cells, and physical barriers can significantly alter network conditions. A responsive network can quickly modify its operational parameters, including beamforming vectors [32, 19, 23, 20, 11, 14], power levels [30, 13, 25, 8, 17], and frequency bands, to counter these challenges and maintain peak performance.

In DFRC systems, the demand for adaptability and responsiveness is even more pronounced. Operating in the high-frequency mmWave bands, these systems face challenges such as obstacle sensitivity and rapid signal decay over distances. The dual-function nature of these systems, serving both radar sensing and communication, adds another layer of complexity. They must manage communication needs while ensuring the radar's operational effectiveness for applications like target detection and tracking.

The implementation of rapid algorithms in DFRC systems marks a significant advancement in tackling these challenges. By adjusting the beamforming weights and incorporating the reliability of phased array elements, these algorithms enable the system to quickly respond to shifts in user demands, environmental changes, and structural integrity. This approach ensures that the system is proactive in maintaining service quality, operational efficiency, and reliability.

The necessity for adaptability and responsiveness in modern cellular networks, especially in DFRC systems, is not merely a requirement; it is a defining characteristic that determines their operational effectiveness and future readiness. As user requirements and operational challenges continue to grow, the ability of these networks to dynamically adjust and respond will be crucial for their success and sustainability.

Proportional fairness has traditionally been a fundamental concept in communication system design, aiming to balance resource allocation among users based on their needs. However, in modern cellular systems where users have varied QoS demands and different modulation schemes, traditional proportional fairness may lead to inefficiencies. For instance, allocating the same bandwidth to both a high-definition video stream and a simple IoT sensor transmission can result in resource waste. The video may require more bandwidth for optimal performance, while the IoT data might not utilize its share fully.

The concept of utility proportional fairness, which focuses on maximizing user satisfaction or the effectiveness of re-

Anis Hamadouche and Mathini Sellathurai are with the School of Engineering & Physical Sciences, Heriot-Watt University, Edinburgh EH14 4AS, UK (e-mail: {ah225,ah2161,m.sellathurai}@hw.ac.uk). Christos Masouros is with the Institute of Communications and Connected Systems, University College London, UK (e-mail: c.masouros@ucl.ac.uk). Tharm Ratnarajah and John Thompson are with the School of Engineering, University of Edinburgh, Edinburgh, EH9 3BF, UK (e-mail: T.Ratnarajah, jst@ed.ac.uk@ed.ac.uk).

source allocation per user, is more suitable in such diverse settings. It ensures that each user receives an appropriate share of resources based on their specific QoS demands and modulation capabilities, thereby optimizing overall network efficiency and user experience.

In traditional beamforming configurations, the power distribution across the antenna array often overlooks the varying condition and reliability of individual antenna elements. This neglect can result in power being directed towards compromised or less reliable elements, thereby reducing overall system performance and increasing the risk of failures. However, by incorporating a reliability matrix for the phased array elements into the beamforming optimization process, the system can identify and evaluate the reliability of each element, adjusting power allocation accordingly.

This method results in the development of a sparse beamforming matrix, which strategically focuses transmission power on the more reliable elements within the array. By concentrating power on these dependable elements, the system significantly enhances its resilience against failures or degradation of its components. In cases of structural damage or progressive wear, this adaptive approach allows the system to dynamically recalibrate its power distribution, continually adapting to the changing conditions of the antenna array.

The benefits of this approach are multifaceted. Firstly, it increases overall system reliability by effectively circumventing or minimizing the impact of unreliable or damaged elements. Secondly, it boosts fault tolerance, ensuring that the system retains operational integrity and continues to perform to expected standards even when some elements are compromised. This level of resilience is especially vital in critical scenarios, such as in essential communication infrastructures or defense applications where uninterrupted operation is crucial.

Moreover, integrating structural sparsity knowledge into the beamforming design fosters the development of more intelligent and adaptive Dual Function Radar Communication (DFRC) systems. By enabling the system to self-assess and dynamically adapt to its structural health, this approach introduces an element of self-awareness and self-optimization. This represents a significant step towards the realization of smarter, more autonomous communication systems.

Our contributions in dual-functional radar-communication (DFRC) systems are characterized by:

- The introduction of a new array selection criterion that integrates antenna-health information for beam pattern correction and enhancing system reliability;
- introducing simple, lightweight, optimization techniques like proximal-gradient dual ascent for directly tackling nonconvex challenges in sparse array selection without unnecessary mathematical relaxation;

The paper is systematically organized into six main sections to provide a comprehensive exploration of the research topic. Section II, "Related Work", lays the foundational groundwork by reviewing pertinent literature, thereby contextualizing our study within the broader scope of existing research in Dual Function Radar Communication (DFRC) systems. In Section III, "Problem Formulation", we formulate the

joint radar-communication beamforming problem as an optimisation problem and introduce the mathematical system models, detailing the complexities and setting the stage for the subsequent discussion of our proposed methodologies. In Section IV, "Antenna-Health Aware Beamforming", we introduce the Proximal-Gradient Dual Ascent (PGDA) algorithm, emphasizing its adaptiveness and efficiency in managing spectral resources and maintaining system reliability. Section V, "Experimental Results", presents a rigorous evaluation of our proposed solutions, substantiating our theoretical claims with empirical data and insightful analysis. Finally, Section VI, "Conclusion", encapsulates the key findings, discusses the implications of our research, and offers a perspective on potential future directions in the realm of DFRC systems.

II. RELATED WORK

In the area of hybrid beamforming for dual-functional radar-communication (DFRC) systems, significant progress has been documented by Cheng et al. [16] and Qi et al. [24]. Cheng et al. developed a framework for multi-carrier DFRC systems that concentrates on maximizing sum-rate subject to power and similarity constraints. Qi et al. expanded these principles to mmWave MIMO integrated sensing and communication (ISAC) systems, aiming to optimize transmit beams at DFRC base stations while accommodating communication user constraints.

Tian et al. [18] explored the optimization of transmit/receive beamforming for MIMO-OFDM based DFRC systems, focusing on quality of service (QoS) and transmit power constraints with Kullback-Leibler divergence as a key metric. Liu et al. [12] introduced a MIMO beamforming design that seeks to minimize the mean squared error (MSE) of target estimation while maintaining satisfactory user signal-to-interference-plus-noise ratios (SINRs).

Further enhancements in beamforming and system optimization are presented by Wang et al. [27], Wei et al. [28], and Li et al. [22]. Wang et al. tackled low-complexity beamforming designs within a MIMO radar and multi-user communication framework. Wei et al. examined an IRS-aided DFRC system, orchestrating radar receive filters, frequency-dependent beamforming, and IRS phases jointly. Li et al. devised an optimization strategy for both transmit beamforming and receive filter design in a two-cell DFRC network.

Significant advancements in predictive beamforming are credited to Yuan et al. [15], Liu et al. [10], and Yu et al. [35]. Yuan et al. introduced a predictive beamforming scheme for vehicular networks aiming to minimize signaling overhead and enhance tracking performance. Liu et al. discussed predictive beamforming for V2I links without relying on explicit state evolution models. Yu et al. proposed a neural network-based method for angle estimation in multi-RSU vehicular networks.

Tian et al. [26] explored adaptive bit/power allocation alongside beamforming to improve BER performance in DFRC systems. Liu et al. [11] focused on radar-assisted predictive beamforming for vehicular links, using DFRC signals for enhanced vehicle tracking.

Further deep dives into hybrid beamforming include Cheng et al. [16] and Dai et al.'s work on OFDM-DFRC and SINR

metric-based DFRC systems, respectively, tackling nonconvex challenges using consensus-ADMM and SDR techniques. Cheng et al. [20] proposed a double-phase-shifter based hybrid beamforming approach for mmWave DFRC systems using consensus-ADMM and WMMSE to overcome nonconvex issues.

Xu et al. [33] applied learning techniques, particularly neural networks, to optimize transmit beamforming, addressing the nonconvex nature of these challenges. Liang and Huang [31] used online learning networks to design nonconvex joint transmit waveform and receive beamforming in DFRC systems.

Additionally, recent contributions include Xu et al. (2023) [34] and Wu et al. (2022) [29], focusing on antenna selection technologies in massive MIMO systems for 5G networks and sparse array design in joint communication radar systems, respectively. These efforts aim at optimizing the ambiguity function for better radar detection while maintaining communication quality of service.

In contrast to the existing methods, our approach offers a more integrated and adaptive solution for beamforming and array selection in DFRC systems. Employing a new array selection criterion that incorporates system health data into the optimization process, our method utilizes proximal-gradient dual ascent for effective nonconvex challenge resolution. This approach ensures faster convergence and superior adaptability to dynamic conditions, making it ideal for real-time applications in fluctuating environments. Moreover, it achieves an optimal balance between radar and communication goals, ensuring proportional fairness and meeting minimum rate requirements across communication users, thereby enhancing both system performance and network equity.

III. PROBLEM FORMULATION

Consider a millimeter wave (mmWave) Dual-Function Radar Communications (DFRC) node equipped with N_t transmit antennas and N_r receive antennas. This node services M users, each having a single antenna, while concurrently tracking K point targets. Assume \mathbf{X} represents the dual-function narrow-band transmit matrix of dimensions $N_t \times L$, expressed as:

$$\mathbf{X} = \mathbf{W}\mathbf{S} \quad (1)$$

where $L > N_t$ is the duration of the DFRC signal frames, $\mathbf{W} = [\mathbf{w}_1, \dots, \mathbf{w}_M]^T$ is the beamforming matrix that needs designing with \mathbf{w}_j being the j -th beamforming vector, and $\mathbf{S} \in \mathbb{C}^{M \times L}$ represents the data stream.

We assume that these data streams are independent, hence

$$\frac{1}{L} \mathbf{S}\mathbf{S}^H = \mathbf{I}_{N_t} \quad (2)$$

This equation holds asymptotically when the signaling adopts a Gaussian distribution and L is sufficiently large.

Equation (2) demonstrates that the data streams remain orthogonal throughout the frame's duration L , ensuring no interference occurs among them. This orthogonality is a common stipulation in numerous communication systems to prevent interference across different data streams. The term

on the right, \mathbf{I}_{N_t} , denotes the identity matrix for size N_t , indicating that when the data streams are cross-multiplied with their Hermitian transposes (\mathbf{S}^H), they yield an identity matrix, scaled by the length of the frame L .

A. Radar system Model

The matrix \mathbf{Y}^r , representing the signals reflected by the target and received by the antennas, is of dimension $N_r \times L$. It is defined as:

$$\mathbf{Y}^r = \mathbf{G}\mathbf{X} + \mathbf{\Omega} \quad (3)$$

where $\mathbf{G} \in \mathbb{C}^{N_r \times N_t}$ denotes the target response matrix and $\mathbf{\Omega} \in \mathbb{C}^{N_r \times L}$ is the matrix of additive white Gaussian noise (AWGN), each element having a variance σ_r^2 .

For a collocated MIMO radar, the target response matrix is defined as:

$$\mathbf{G} = \sum_{k=1}^K \alpha_k \mathbf{a}(\theta_k) \mathbf{b}^H(\theta_k) \quad (4)$$

In this expression, α_k reflects the complex coefficient representing both the two-way channel amplitude and the radar cross-section of the k -th target. θ_k signifies both the angle of departure (AoD) and angle of arrival (AoA) of the k -th target, under the assumption that transmitter and receiver antennas are collocated.

The steering vectors for the transmit and receive antennas are given by:

$$\mathbf{a}(\theta) = \left[1, e^{j\frac{2\pi}{\lambda}d \sin(\theta)}, \dots, e^{j\frac{2\pi}{\lambda}d(N_t-1) \sin(\theta)} \right]^T \quad (5)$$

$$\mathbf{b}(\theta) = \left[1, e^{j\frac{2\pi}{\lambda}d \sin(\theta)}, \dots, e^{j\frac{2\pi}{\lambda}d(N_r-1) \sin(\theta)} \right]^T \quad (6)$$

where λ is the wavelength of the signal, and d represents the spacing between antennas.

For the purposes of this discussion, we assume that $d = \frac{\lambda}{2}$. Hence, the covariance of the radar channel can be expressed as:

$$\mathbf{R} = \sum_{k=1}^K \sigma_k^2 (\mathbf{b}(\theta_k) \otimes \mathbf{a}(\theta_k)) (\mathbf{b}(\theta_k) \otimes \mathbf{a}(\theta_k))^H \quad (7)$$

where $\sigma_k^2 = \mathbb{E}[\alpha_k \alpha_k^H]$ represents the expected power strength of the k -th target.

The mutual information between the received echo signal \mathbf{Y}^r and the radar channel \mathbf{G} , denoted as $I(\mathbf{Y}^r; \mathbf{G})$, is calculated as:

$$I(\mathbf{Y}^r; \mathbf{G}) = H(\mathbf{Y}^r) - H(\mathbf{Y}^r | \mathbf{G}) = \log \det(\mathbf{I}_{N_r} + \sigma_r^{-2} \mathbf{R} \mathbf{X} \mathbf{X}^H) \quad (8)$$

Here, $H(\mathbf{Y})$ represents the differential entropy of \mathbf{Y} , where $P(\mathbf{Y})$ is its probability density function (PDF), and $H(\mathbf{Y} | \mathbf{G})$ signifies the conditional differential entropy given \mathbf{G} . The identity $\det(\mathbf{I} + \mathbf{A}\mathbf{B}) = \det(\mathbf{I} + \mathbf{B}\mathbf{A})$ is used to derive equation (6).

In the next subsection, we will proceed to outline the communication model.

B. Communication system model

The received communication signal $\mathbf{Y}^c \in \mathbb{C}^{M \times L}$ for a scenario involving a single target is described by:

$$\mathbf{Y}^c = \mathbf{H}^H \mathbf{X} + \mathbf{N}, \quad (9)$$

where $\mathbf{N} \in \mathbb{C}^{M \times L}$ represents the additive white Gaussian noise (AWGN) matrix, each element possessing a variance σ_c^2 . Furthermore, $\mathbf{H} = [\mathbf{h}_1, \dots, \mathbf{h}_M] \in \mathbb{C}^{N_t \times M}$ denotes the communication channel matrix, with $\mathbf{h}_j \in \mathbb{C}^{N_t}$ indicating the channel corresponding to the j -th user. The signal-to-interference-plus-noise ratio (SINR) for the m -th user is then calculated as:

$$\gamma_m = \frac{|\mathbf{h}_m^H \mathbf{w}_m|^2}{\sum_{j \neq m} |\mathbf{h}_m^H \mathbf{w}_j|^2 + \sigma_c^2}, \quad (10)$$

in which the term $\sum_{j \neq m} |\mathbf{h}_m^H \mathbf{w}_j|^2$ quantifies the interference from other users affecting the m -th user.

C. Antenna-Health constraints

In a phased array system equipped with N antenna elements and M RF chains, the interactions between these components—mediated through beamforming weights that adjust phase and amplitude—are encapsulated by a matrix β with dimensions $N \times M$. This matrix represents the health and operational status of each antenna element in relation to the RF chains. Each element, $\beta_{i,j}$, within the matrix indicates the reliability or operational health of the connection between the i -th RF chain and the j -th antenna element, with values ranging from 0 (denoting complete failure or an off state) to 1 (indicating full operational status). This reliability measure can encompass the operational integrity of individual components such as power amplifiers, attenuators, phase shifters, or directly reflect the antenna elements' reliability. In cases where only the antenna elements are considered, β reduces to a vector of length N , where each β'_i , for $i = 1, \dots, N$, quantifies the reliability of the i -th antenna element. Here, N represents the total number of antenna elements, denoted as N_t for transmitters and N_r for receivers.

Assessing system reliability involves a multifaceted process that includes simulations, far-field and near-field measurements, network analysis, and environmental testing. These measures are designed to identify and mitigate potential performance degradations. Continuous monitoring and advanced correction algorithms are crucial to maintain the efficiency and reliability of phased array systems.

The following section will discuss strategies to jointly maximize the radar's mutual information and the minimum quality of service (QoS) of the communication users while considering power limitations and antenna health constraints.

IV. ANTENNA-HEALTH AWARE BEAMFORMING

In practical applications, incorporating the reliability data of phased array elements into the beamforming optimization problem marks a significant evolution towards more robust, dependable, and fault-tolerant DFRC systems. This method optimizes resource utilization by directing power towards the

most reliable elements, thereby guaranteeing continuous and efficient operation even amidst structural challenges. Such an approach not only enhances system resilience but also establishes a new benchmark in the design and functioning of sophisticated communication systems.

A. Antenna-health aware selection

The optimization problem in question aims to enhance joint radar-communication (JRC) systems by maximizing radar performance and ensuring efficient hardware usage, particularly focusing on systems with N_t antenna elements serving M users. The objective function is twofold: firstly, it seeks to amplify radar functionality through the mutual information (MUI); secondly, it aims to minimize hardware complexity by reducing the use of less reliable antennas, weighted by ρ_s , penalizing those with compromised functionality ($\beta'_i \neq 1$). The optimization is subject to constraints that limit the total power consumption to a specified budget P_{tot} and ensure that the minimum data rate R_{\min_j} is met for all users. Definitions crucial to the problem include w_i^r and w_j^c , denoting i -th beamforming row vector weights per antenna and the j -th beamforming vector weights per communication channel, respectively, along with ρ_r and ρ_s as weighting factors for radar performance and sparsity (prior information). The health status of each antenna is indicated by β'_i .

The constrained optimisation problem can be formalised as follows:

$$\max_{\mathbf{w}_j, \forall j} \quad \rho_r \log \det \left(\mathbf{I}_{N_t} + \sigma_r^{-2} \mathbf{R} \sum_{j=1}^M \mathbf{w}_j \mathbf{w}_j^H \right) \quad (11a)$$

$$\text{subject to} \quad \begin{aligned} & -\rho_s \sum_{i=1}^{N_t} (1 - \beta'_i) \|\mathbf{w}_i^r\|_2 \\ & \frac{\sum_{j=1}^M \|\mathbf{w}_j^c\|_2^2}{\eta} + P_A \sum_{i=1}^{N_t} \|\mathbf{w}_i^r\|_2 \leq P_{tot}, \end{aligned} \quad (11b)$$

$$R_{\min_j} \leq \log(1 + \gamma_j), \quad \forall j, \quad (11c)$$

where \mathbf{I}_{N_t} is the identity matrix, η denotes the efficiency of power amplifiers, P_A the power associated with active antennas, and γ_j the SINR for the j -th user. The sparsity promoting term $\rho_s \sum_{i=1}^{N_t} (1 - \beta'_i) \|\mathbf{w}_i^r\|_2$ provides a metric for the operational status of each antenna i , guiding the optimization towards utilizing fully functional antenna elements. Constraint (11b) includes not just the transmit power $\sum_{j=1}^M \|\mathbf{w}_j^c\|_2^2 / \eta$ but also accounts for the energy used by the power amplifiers, digital-to-analog converters (DACs), and other RF chain components $P_A \sum_{i=1}^{N_t} \|\mathbf{w}_i^r\|_2$, encapsulating the system's overall energy footprint (see Appendix C for full power model).

This optimization framework strategically balances enhancing radar detection capabilities, fulfilling communication requirements, and optimizing hardware employment, reinforcing the efficiency and reliability of DFRC system designs.

Given the constrained optimization problem, we apply the group proximal-gradient dual ascent whose implementation is

given in Algorithm 1, where the Lagrangian \mathcal{L} , the gradient $\nabla_{\mathbf{w}}\mathcal{L}$ and the proximal $\text{prox}_{(\rho_s(1-\text{beta}'_i)+\lambda P_A)\|\cdot\|_2}$ are given in Appendix D.

Algorithm 1 Group Proximal-Gradient Dual Ascent (GPGDA) For Antenna Selection

- 1: **initialize** \mathbf{w}_j for all j , λ , μ_j for all j , step sizes α and η
 - 2: **while** not converged **do**
 - 3: Compute gradient $\nabla_{\mathbf{w}}\mathcal{L}$
 - 4: Update \mathbf{w} using gradient step: $\mathbf{w} \leftarrow \mathbf{w} + \eta\nabla_{\mathbf{w}}\mathcal{L}$
 - 5: **for** each beamforming row \mathbf{w}_i^r **do**
 - 6: Update group row \mathbf{w}_i^r using the proximal operator:
 - 7: $\mathbf{w}_i^r \leftarrow \text{prox}_{(\rho_s(1-\text{beta}'_i)+\lambda P_A)\|\cdot\|_2}(\mathbf{w}_i^r)$
 - 8: **end for**
 - 9: Update dual variable λ for power constraint:
 - 10: $\lambda \leftarrow \lambda + \alpha \left(\frac{\sum_{j=1}^M \|\mathbf{w}_j^c\|_2^2}{\eta} + P_A \sum_{i=1}^{N_t} \|\mathbf{w}_i^r\|_2 - P_{tot} \right)$
 - 11: **for** each user j **do**
 - 12: Update dual variable μ_j for minimum rate constraint:
 - 13: $\mu_j \leftarrow \mu_j + \alpha (R_{\min,j} - \log(1 + \gamma_j))$
 - 14: **end for**
 - 15: Check for convergence
 - 16: **end while**
-

B. Time complexity

The Group Proximal-Gradient Dual Ascent (GPGDA) algorithm involves several computationally intensive steps that collectively determine its overall efficiency and effectiveness, particularly when applied to large-scale systems. The analysis of each step's computational complexity gives insight into potential bottlenecks and areas where performance enhancements might be necessary.

First, the gradient computation (see Appendix A) within the GPGDA algorithm is crucial, as it directly impacts the rate of convergence and overall effectiveness. This step involves the multiplication of a matrix X of dimensions $N_t \times M$ with its Hermitian transpose X^H , resulting in an $N_t \times N_t$ matrix. This operation alone has a complexity of $O(N_t^2 \times M)$, which can be substantial in systems where N_t and M are large. Furthermore, the subsequent addition of this product to an identity matrix followed by inversion of the resultant matrix introduces a complexity of $O(N_t^3)$ due to the matrix inversion. This inversion is typically the most computationally demanding operation within the algorithm, dominating the per-iteration complexity.

The algorithm then updates the beamforming matrix \mathbf{w} using a gradient step, which scales linearly with the size of the matrix, $O(N_t \times M)$. Additionally, the proximal operator is applied to each row of \mathbf{w} , with each application having a complexity of $O(M)$, leading to an overall row update complexity of $O(N_t \times M)$. Although these operations are less complex than the matrix inversion, they still contribute significantly to the workload, especially in larger matrices.

The dual variables are also updated within each iteration. The power constraint dual variable λ update involves operations scaling with $O(N_t \times M)$, and the updates for the

minimum rate constraints for each user μ_j scale with $O(M)$. These updates, while generally less complex than the matrix operations, are critical for ensuring the algorithm adheres to system constraints and optimizes performance.

In summary, the most computationally intense phase of each iteration of the GPGDA algorithm is the gradient computation (see Appendix A), particularly the matrix inversion, which operates with a complexity of $O(N_t^3)$. When considering the number of iterations K needed for the algorithm to converge, the total complexity amounts to $O(K \times N_t^3)$. This significant computational demand underscores the importance of using efficient computational techniques and possibly specialized hardware to handle these operations, particularly in real-time applications where speed and efficiency are crucial. The algorithm's complexity indicates that it is best suited for scenarios where the benefits of optimized beamforming significantly outweigh the computational costs.

C. Power consumption of GPGDA

To calculate the total power consumption per iteration for the Group Proximal-Gradient Dual Ascent (GPGDA) algorithm, it is crucial to consider the power consumed in each computational step. In the gradient computation step (see Appendix A), which includes the multiplication of an $N_t \times M$ matrix by its $M \times N_t$ Hermitian transpose, there are $N_t^2 \times M$ multiplications and $N_t^2 \times (M-1)$ additions involved. Additionally, the matrix inversion operation, which typically follows, comprises N_t^3 multiplications and N_t^3 additions. Therefore, the power required for these gradient-related calculations sums up to $N_t^2 \times M \times P_{\times} + N_t^3 \times P_{\times}$ for the multiplications, and $N_t^2 \times (M-1) \times P_{+} + N_t^3 \times P_{+}$ for the additions.

Following the gradient calculation, updating the beamforming matrix \mathbf{w} using a gradient step involves $N_t \times M$ multiplications and the same number of additions, translating to $N_t \times M \times P_{\times}$ and $N_t \times M \times P_{+}$, respectively. The proximal operation executed on each row of \mathbf{w} includes norm calculations and vector multiplications (ignoring the comparator's power $P_{<,>}$), which contribute further to the power expenditure: each of the N_t rows requires $2M$ multiplications and M additions, resulting in a total of $2N_t \times M \times P_{\times}$ and $N_t \times M \times P_{+}$. Dual variable updates for power and rate constraints also require operations proportional to the dimensions of \mathbf{w} , adding $N_t \times M \times P_{\times}$ and $N_t \times M \times P_{+}$ for multiplications and additions, respectively. Summing all these contributions, the total power consumption per iteration of the algorithm is given by $((N_t^2 \times M + N_t^3 + 5N_t \times M) \times P_{\times}) + ((N_t^2 \times M + N_t^3 + 3N_t \times M - N_t^2) \times P_{+})$, illustrating the significant energy demands of the operations, especially those involving matrix calculations.

This analysis highlights the importance of optimizing computational efficiency in the implementation of the GPGDA algorithm, especially for systems where energy efficiency is paramount. However, for the sake of simplicity, we do not consider the algorithmic power consumption in the following experiments.

V. EXPERIMENTAL RESULTS

Assuming a spectrum sharing scenario within the 28GHz band (5G mmWave), a strategic allocation is made where

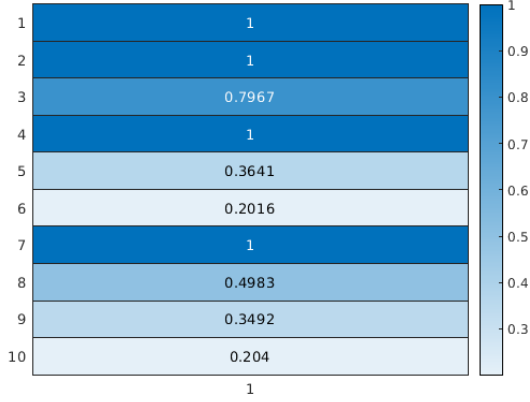


Fig. 1: Linear Array Antenna Reliability Vector

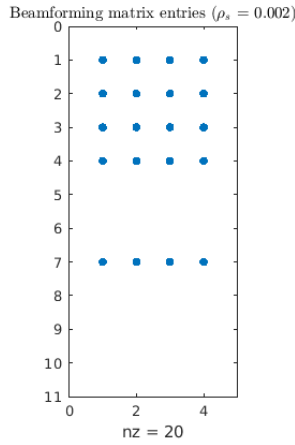


Fig. 2: 50%-sparse beamforming weight matrix solution for $\rho_s = 0.001$.

0.4140 GHz (with a proportion, $\rho_r = 0.0148$), is dedicated to radar usage, while significant sub-bands, specifically 5.6906 GHz, 7.6838 GHz, 7.6128 GHz, and 6.5987 GHz (with respective proportions $\rho = [0.2032, 0.2744, 0.2719, 0.2357]$), are allocated to 5G communication users. This allocation underlines the coexistence strategy of radar and 5G communications in the same frequency band, aiming to optimize the spectrum utilization. The system adheres to strict quality of service (QoS) requirements, ensuring a minimum of 100Mbps data rate for each 5G user within a maximum power budget of 100 Watts. This operational framework translates into specific spectral efficiencies, with minimum spectral efficiency denoted as $R_{min} = [0.0176, 0.0130, 0.0131, 0.0152]$.

In this experiment we use the reliability of antenna elements of Figure 1 to guide the selective beamforming optimisation algorithm to select the most reliable antenna elements subject to a minimum communication rate of 100 Mbps and a total power budget of 100 Watts with power efficiency of 0.4 and per-antenna element power of $P_A = 5$ Watts (for simplicity). Table I summarises the results of our experiments and the antenna selection (non-zero rows) is depicted in Figures 2-3 for different sparsity promotion weights (ρ_s).

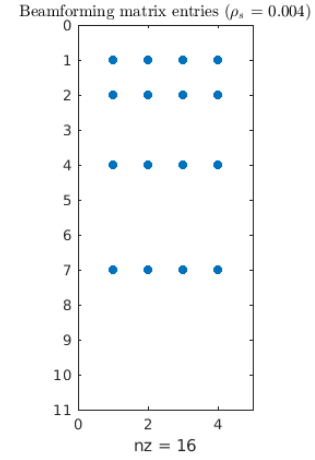


Fig. 3: 40%-sparse beamforming weight matrix solution for $\rho_s = 0.002$.

ρ_s	Avg. SE (bps/Hz)	Avg. R (Gbps)	RL (%)	MUI	DENS (%)	PW (W)
0	0.1941	1.2763	0.21	22.5190	100	100.0283
0.0008	0.3202	2.0597	1.02	21.8759	90	94.4355
0.0015	0.4827	3.2399	79.67	21.4898	50	97.6907
0.0023	0.3159	2.4701	79.67	21.4933	50	100.0094
0.0031	0.3854	4.3085	79.67	21.4140	50	99.9730
0.0038	0.5033	5.0732	100.0	21.3089	40	100.0466
0.0061	0.1987	1.6519	100.0	21.3097	40	99.9578
0.0767	0.2621	0.9520	100.0	21.3121	40	100.0029

TABLE I: Summary of System Performance Metrics

Table I shows the performance of a DFRC system under varying levels of sparsity promotion weight (ρ_s). Notably, as ρ_s increases, there are significant changes in several key performance metrics of the system.

Initially, when ρ_s is at 0, the average spectral efficiency (SE) and data rate (R) are low, while the beamforming matrix is fully dense (100%). The system reliability (RL) is extremely low (0.21%), and the mutual information for radar (MUI) is at its highest. As ρ_s is increased to 0.0038, both the SE and R notably improve, peaking at values of 0.5033 bps/Hz and 5.0732 Gbps, respectively. This peak performance in SE and R corresponds with perfect system reliability (100%), which starts being achieved consistently at ρ_s values of 0.0038 and higher. It is interesting to note that the beamforming matrix density (DENS) decreases to 40% as ρ_s increases, suggesting a more sparse matrix that presumably focuses power more effectively despite the lower overall transmission power (PW), which remains around 100 W.

However, after reaching a peak at ρ_s of 0.0038, both SE and R experience a decline at higher values of ρ_s despite maintained reliability and further reduction in MUI. For instance, at ρ_s of 0.0767, the SE and R drop to 0.2621 bps/Hz and 0.9520 Gbps, respectively, which are lower than the initial values at $\rho_s = 0$. This suggests that while higher sparsity can enhance system efficiency up to a point, excessive sparsity may degrade performance, highlighting the need for a balanced approach to the sparsity promotion in beamforming matrix design for optimizing overall system performance.

VI. CONCLUSION

Our investigation into integrating phased array elements' reliability matrix into beamforming design has confirmed significant benefits of sparse selective beamforming. The study demonstrates that adjusting ρ_s , the sparsity promotion weight, substantially enhances system performance metrics such as spectral efficiency and data rate, ensuring high system reliability. Optimal performance was noted at an intermediate ρ_s value, beyond which increased sparsity led to diminished returns. This finding indicates a critical threshold for effective sparsity application. Moreover, the implementation of GPGDA methods has successfully tackled complex nonconvex optimization challenges in sparse array configurations. This research provides a strong foundation for future advancements in Dual Function Radar Communication (DFRC) and Integrated Sensing and Communication (ISAC) systems, propelling them towards greater intelligence and adaptability. Furthermore, while this study did not delve into specific algorithmic power consumption details, recognizing the significance of energy efficiency in such algorithms is essential, particularly for deployment in resource-constrained environments. Future research should focus on a comprehensive evaluation of algorithmic power demands to enhance the sustainability and practicality of these advanced beamforming techniques.

APPENDIX

A. Gradient of radar detection mutual information term

To find the gradient of $A(X) = \log \det(I_{N_t} + \sigma_r^{-2} R X X^H)$ with respect to X , we can utilize the matrix derivative identity:

$$\frac{\partial \log \det(F(X))}{\partial X} = F(X)^{-1} \frac{\partial F(X)}{\partial X}$$

Given:

$$A(X) = \log \det(Y)$$

where $Y = I_{N_t} + \sigma_r^{-2} R X X^H$,

Let us differentiate $A(X)$ with respect to the matrix X :

$$\frac{\partial A(X)}{\partial X} = \text{trace} \left(Y^{-1} \frac{\partial Y}{\partial X} \right)$$

Now, differentiating Y with respect to X :

$$\frac{\partial Y}{\partial X} = \sigma_r^{-2} R \frac{\partial (X X^H)}{\partial X}$$

Considering $X X^H$, the derivative w.r.t. X would introduce a term that depends on X^H . Therefore, using the identity for differentiation of a product:

$$\frac{\partial (X X^H)}{\partial X} = X^H$$

Combining the above expressions:

$$\frac{\partial A(X)}{\partial X} = \text{trace} (Y^{-1} \sigma_r^{-2} R X^H)$$

This gives the gradient of $A(X)$ with respect to X .

If we want to differentiate the outer product of $\mathbf{w}(1 : M)$ with its Hermitian transpose, i.e.,

$$\mathbf{w}(1 : M) \mathbf{w}^H(1 : M)$$

with respect to a specific element product $w_i w_k^*$, let us derive that.

Let us first note what the matrix product looks like:

$$\mathbf{w}(1 : M) \mathbf{w}^H(1 : M) = \begin{bmatrix} |w_1|^2 & w_1 w_2^* & \dots & w_1 w_M^* \\ w_2 w_1^* & |w_2|^2 & \dots & w_2 w_M^* \\ \vdots & \vdots & \ddots & \vdots \\ w_M w_1^* & w_M w_2^* & \dots & |w_M|^2 \end{bmatrix}$$

We are interested in the gradient with respect to the element $w_i w_k^*$ (where i and k are given indices).

The only places in this matrix where w_i and w_k^* multiply together are in the (i,k) and (k,i) positions. Everywhere else, differentiating with respect to $w_i w_k^*$ will give zero.

Differentiating the (i,k) position:

$$\frac{\partial (w_i w_k^*)}{\partial (w_i w_k^*)} = 1$$

Because the element in (i,k) is $w_i w_k^*$.

Differentiating the (k,i) position:

$$\frac{\partial (w_k w_i^*)}{\partial (w_i w_k^*)} = 1$$

Because the element in (k,i) is $w_k w_i^*$, which is the conjugate of $w_i w_k^*$, and its derivative with respect to $w_i w_k^*$ is also 1.

For all other positions in the matrix, the derivative is zero.

So, the matrix of derivatives (or the Jacobian) for the element $w_i w_k^*$ is:

$$\frac{\partial \mathbf{w}(1 : M) \mathbf{w}^H(1 : M)}{\partial (w_i w_k^*)} = \begin{bmatrix} 0 & \dots & 0 & \dots & 0 \\ \vdots & \ddots & \vdots & \ddots & \vdots \\ 0 & \dots & 1 & \dots & 0 \\ \vdots & \ddots & \vdots & \ddots & \vdots \\ 0 & \dots & 0 & \dots & 0 \end{bmatrix}$$

Where the only non-zero entries are at the (i,k) and (k,i) positions, which are both 1.

B. Gradient of communication term

Let us use the gradient ascent for the \mathbf{x} -update. To find the partial derivative of $\sum_{m=1}^M \log(1 + \gamma_m)$ with respect to $w_{i,k}$, we will use the chain rule. Given that γ_m has a specific functional form in terms of $w_{i,k}$, we can express the derivative as:

$$\frac{\partial \sum_{m=1}^M \log(1 + \gamma_m)}{\partial w_{i,k}} = \sum_{m=1}^M \frac{1}{1 + \gamma_m} \frac{\partial \gamma_m}{\partial w_{i,k}} \quad (12)$$

where

$$\frac{\partial \gamma_m}{\partial w_{i,k}} = \begin{cases} \frac{\mathbf{h}_m \mathbf{h}_m^H \mathbf{w}_m + \mathbf{h}_m \mathbf{h}_m^H \mathbf{w}_m^*}{\sum_{j \neq m} |\mathbf{h}_m^H \mathbf{w}_j|^2 + \sigma_c^2} & \text{if } i = m \\ \frac{|\mathbf{h}_m^H \mathbf{w}_m|^2 \mathbf{h}_m \mathbf{h}_m^H \mathbf{w}_i + \mathbf{h}_m \mathbf{h}_m^H \mathbf{w}_i^*}{(\sum_{j \neq i} |\mathbf{h}_i^H \mathbf{w}_j|^2 + \sigma_c^2)^2} & \text{if } i \neq m \end{cases} \quad (13)$$

or

$$\frac{\partial \gamma_m}{\partial w_{i,k}} = \begin{cases} \frac{\mathbf{h}_m \mathbf{h}_m^H \mathbf{w}_m + \mathbf{h}_m \mathbf{h}_m^H \mathbf{w}_m^*}{\sum_{j \neq m} |\mathbf{h}_m^H \mathbf{w}_j|^2 + \sigma_c^2} & \text{if } i = m \\ \gamma_m \frac{\mathbf{h}_m \mathbf{h}_m^H \mathbf{w}_i + \mathbf{h}_m \mathbf{h}_m^H \mathbf{w}_i^*}{\sum_{j \neq i} |\mathbf{h}_i^H \mathbf{w}_j|^2 + \sigma_c^2} & \text{if } i \neq m \end{cases} \quad (14)$$

C. Power Consumption Model for Phased Array Systems

Designing an energy-efficient phased array system for simultaneous radar and communication functionalities demands a comprehensive understanding and integration of a detailed power consumption model. This model incorporates the efficiency of power amplifiers (PAs), the consumption characteristics of digital-to-analog converters (DACs), and the overall energy requirements of RF chain components, alongside the aggregate transmit power. Specifically, the total transmit power (P) is quantified as the sum of the squared magnitudes of the beamforming weights (w_k) for each user, mathematically expressed as

$$P = \sum_{k=1}^M \|w_k\|_2^2. \quad (15)$$

The power output of PAs, crucial for amplifying the transmitted signals, is directly tied to the transmit power and PA efficiency (η), with

$$P_{PA} = \frac{P}{\eta}. \quad (16)$$

DACs, essential for converting digital signals into analog, consume power as a function of their resolution (q), sampling rate (f), and specific power consumption coefficients (c_1 for static and c_2 for dynamic consumption), resulting in

$$P_{DAC} = c_1 f q + c_2 2^q. \quad (17)$$

Additionally, the power consumption attributable to RF chain components, including mixers (P_M), low-pass filters (P_{LF}), and hybrids with buffers (P_{HB}), sums up to

$$P_{RF} = 2P_M + 2P_{LF} + P_{HB}. \quad (18)$$

Consequently, the total power consumption at the base station (P_{tot}) encapsulates the contributions from the PAs, DACs, and RF components across all N_t antenna elements, following

$$P_{tot} = P_{PA} + N_t(2P_{DAC} + P_{RF}). \quad (19)$$

By strategically selecting parameters such as beamforming weights, DAC resolution, and RF chain components, the model facilitates an optimized design of phased array systems that adeptly balances superior performance, exemplified by optimal SINR, with reduced energy consumption, thereby championing sustainable and economically efficient operations.

D. Group Proximal-Gradient Dual Ascent (GPGDA) For Antenna Selection

To solve the given constrained optimization problem using the proximal-gradient dual ascent method, we first formulate the Lagrangian \mathcal{L} to incorporate both the objective function and the constraints. This method iteratively updates the primal variables (the decision variables \mathbf{w}_j for all j) using proximal-gradient steps for the non-smooth part of the Lagrangian, while the dual variables (λ for the power constraint and μ_j for the minimum rate constraints) are updated using gradient ascent steps to handle the constraints.

The Lagrangian for the given optimization problem integrates the objective function, the power consumption constraint, and the minimum rate constraint as follows:

$$\begin{aligned} \mathcal{L}(\mathbf{w}_j, \lambda, \mu_j) := & \rho_r \log \det \left(\mathbf{I}_{N_t} + \sigma_r^{-2} \mathbf{R} \sum_{j=1}^M \mathbf{w}_j \mathbf{w}_j^H \right) \\ & - \rho_s \sum_{i=1}^{N_t} (1 - \beta_i') \|\mathbf{w}_i^r\|_2 \\ & + \lambda \left(\frac{\sum_{j=1}^M \|\mathbf{w}_j^c\|_2^2}{\eta} + P_A \sum_{i=1}^{N_t} \|\mathbf{w}_i^r\|_2 - P_{tot} \right) \\ & + \sum_{j=1}^M \mu_j (R_{\min_j} - \log(1 + \gamma_j)), \end{aligned} \quad (20a)$$

where ρ_r and ρ_s are the weighting factors for the radar performance and sparsity terms, respectively. \mathbf{w}_j denotes the beamforming vector for the j -th user. \mathbf{w}_i^r and \mathbf{w}_j^c represent the beamforming vectors corresponding to the i -th row and j -th column of the beamforming matrix, respectively. λ and μ_j are the dual variables associated with the power constraint and the minimum rate constraints, respectively.

The optimization process is divided into two main steps:

For the primal variable update, we focus on the non-differentiable part of the Lagrangian, particularly the sparsity-inducing term involving ρ_s . The proximal-gradient step updates the beamforming as follows:

$$\begin{aligned} \mathbf{w}^{(new)} = & \text{prox}_{(\rho_s(1-\beta_i')+\lambda P_A)\|\cdot\|_2} \left(\mathbf{w}^{(old)} + \eta \nabla_{\mathbf{w}} \mathcal{L}(\mathbf{w}^{(old)}, \lambda, \mu_j) \right), \end{aligned} \quad (21)$$

where η is the step size, and $\nabla_{\mathbf{w}_j} \mathcal{L}(\mathbf{w}_j, \lambda, \mu_j)$ is the gradient of the differentiable part of the Lagrangian with respect to \mathbf{w}_j , and $\text{prox}_{(\rho_s(1-\beta_i')+\lambda P_A)\|\cdot\|_2}$ is defined as:

$$\begin{aligned} \text{prox}_{(\rho_s(1-\beta_i')+\lambda P_A)\|\cdot\|_2}(\mathbf{w}_i^r) = & \max \left(1 - \frac{\alpha(\rho_s(1-\beta_i') + \lambda P_A)}{\|\mathbf{w}_i^r\|_2}, 0 \right) \mathbf{w}_i^r \end{aligned} \quad (22)$$

The dual variables are updated using gradient ascent to enforce the constraints. For the power constraint, the update rule is:

$$\lambda^{(new)} = \lambda^{(old)} + \alpha \left(\frac{\sum_{j=1}^M \|\mathbf{w}_j^c\|_2^2}{\eta} + P_A \sum_{i=1}^{N_t} \|\mathbf{w}_i^r\|_2 - P_{tot} \right),$$

and for the minimum rate constraints:

$$\mu_j^{(new)} = \mu_j^{(old)} + \alpha (R_{\min_j} - \log(1 + \gamma_j)),$$

where α is the step size for the dual variable updates.

REFERENCES

- [1] ETP NetWorld2020 et al. “5g: Challenges, research priorities, and recommendations”. In: *Joint White Paper September* (2014).
- [2] Songlin Sun et al. “An intelligent SDN framework for 5G heterogeneous networks”. In: *IEEE Communications Magazine* 53.11 (2015), pp. 142–147.
- [3] Ian F Akyildiz et al. “5G roadmap: 10 key enabling technologies”. In: *Computer Networks* 106 (2016), pp. 17–48.
- [4] Elie BouDaher et al. “Towards a dual-function MIMO radar-communication system”. In: *2016 IEEE Radar Conference (RadarConf)*. IEEE. 2016, pp. 1–6.
- [5] I Chih-Lin et al. “5G: Rethink mobile communications for 2020+”. In: *Philosophical Transactions of the Royal Society A: Mathematical, Physical and Engineering Sciences* 374.2062 (2016), p. 20140432.
- [6] Aboulnahr Hassanien et al. “Non-coherent PSK-based dual-function radar-communication systems”. In: *2016 IEEE Radar Conference (RadarConf)*. IEEE. 2016, pp. 1–6.
- [7] Mansoor Shafi et al. “5G: A tutorial overview of standards, trials, challenges, deployment, and practice”. In: *IEEE journal on selected areas in communications* 35.6 (2017), pp. 1201–1221.
- [8] Ammar Ahmed, Yimin D. Zhang, and Braham Himed. “Distributed Dual-Function Radar-Communication MIMO System with Optimized Resource Allocation”. In: *2019 IEEE Radar Conference (RadarConf)*. 2019, pp. 1–5. DOI: 10.1109/RADAR.2019.8835674.
- [9] Aboulnahr Hassanien et al. “Dual-function radar communication systems: A solution to the spectrum congestion problem”. In: *IEEE Signal Processing Magazine* 36.5 (2019), pp. 115–126.
- [10] Fan Liu and Christos Masouros. “A tutorial on joint radar and communication transmission for vehicular networks—Part III: Predictive beamforming without state models”. In: *IEEE Communications Letters* 25.2 (2020), pp. 332–336.
- [11] Fan Liu et al. “Radar-assisted predictive beamforming for vehicular links: Communication served by sensing”. In: *IEEE Transactions on Wireless Communications* 19.11 (2020), pp. 7704–7719.
- [12] Xiang Liu et al. “Joint transmit beamforming for multiuser MIMO communications and MIMO radar”. In: *IEEE Transactions on Signal Processing* 68 (2020), pp. 3929–3944.
- [13] Chenguang Shi et al. “Joint Optimization of Subcarrier Selection and Power Allocation for Dual-Functional Radar-Communications System”. In: *2020 IEEE 11th Sensor Array and Multichannel Signal Processing Workshop (SAM)*. 2020, pp. 1–5. DOI: 10.1109/SAM48682.2020.9104262.
- [14] Weijie Yuan et al. “Bayesian predictive beamforming for vehicular networks: A low-overhead joint radar-communication approach”. In: *IEEE Transactions on Wireless Communications* 20.3 (2020), pp. 1442–1456.
- [15] Weijie Yuan et al. “Joint radar-communication-based bayesian predictive beamforming for vehicular networks”. In: *2020 IEEE Radar Conference (RadarConf20)*. IEEE. 2020, pp. 1–6.
- [16] Ziyang Cheng, Zishu He, and Bin Liao. “Hybrid beamforming design for OFDM dual-function radar-communication system”. In: *IEEE Journal of Selected Topics in Signal Processing* 15.6 (2021), pp. 1455–1467.
- [17] Chenguang Shi et al. “Joint Optimization Scheme for Subcarrier Selection and Power Allocation in Multicarrier Dual-Function Radar-Communication System”. In: *IEEE Systems Journal* 15.1 (2021), pp. 947–958. DOI: 10.1109/JSYST.2020.2984637.
- [18] Tuanwei Tian et al. “Transmit/receive beamforming for MIMO-OFDM based dual-function radar and communication”. In: *IEEE Transactions on Vehicular Technology* 70.5 (2021), pp. 4693–4708.
- [19] Li Chen et al. “Generalized transceiver beamforming for DFRC with MIMO radar and MU-MIMO communication”. In: *IEEE Journal on Selected Areas in Communications* 40.6 (2022), pp. 1795–1808.
- [20] Ziyang Cheng et al. “Double-phase-shifter based hybrid beamforming for mmwave DFRC in the presence of extended target and clutters”. In: *IEEE Transactions on Wireless Communications* (2022).
- [21] Jeremy Johnston et al. “MIMO OFDM dual-function radar-communication under error rate and beampattern constraints”. In: *IEEE Journal on Selected Areas in Communications* 40.6 (2022), pp. 1951–1964.
- [22] Yiqing Li and Miao Jiang. “Joint Transmit Beamforming and Receive Filters Design for Coordinated Two-Cell Interfering Dual-Functional Radar-Communication Networks”. In: *IEEE Transactions on Vehicular Technology* 71.11 (2022), pp. 12362–12367.
- [23] Rang Liu et al. “Joint transmit waveform and passive beamforming design for RIS-aided DFRC systems”. In: *IEEE Journal of Selected Topics in Signal Processing* 16.5 (2022), pp. 995–1010.
- [24] Chenhao Qi et al. “Hybrid beamforming for millimeter wave MIMO integrated sensing and communications”. In: *IEEE Communications Letters* 26.5 (2022), pp. 1136–1140.
- [25] Tuanwei Tian et al. “Adaptive Bit/Power Allocation With Beamforming for Dual-Function Radar-Communication”. In: *IEEE Wireless Communications Letters* 11.6 (2022), pp. 1186–1190. DOI: 10.1109/LWC.2022.3160674.

- [26] Tuanwei Tian et al. “Adaptive bit/power allocation with beamforming for dual-function radar-communication”. In: *IEEE Wireless Communications Letters* 11.6 (2022), pp. 1186–1190.
- [27] Zhiqin Wang et al. “Low-complexity Transceiver Beamforming for DFRC with MIMO Radar and MU-MIMO Communication”. In: *2022 International Wireless Communications and Mobile Computing (IWCMC)*. IEEE. 2022, pp. 32–37.
- [28] Tong Wei et al. “Simultaneous active-passive beamformer design in IRS-enabled multi-carrier DFRC system”. In: *2022 30th European Signal Processing Conference (EUSIPCO)*. IEEE. 2022, pp. 1007–1011.
- [29] Tongcai Wu, Lina Yuan, and Anran Zhou. “Antenna Selection Technology Research in Massive MIMO System”. In: *2022 IEEE Asia-Pacific Conference on Image Processing, Electronics and Computers (IPEC)*. 2022, pp. 967–970. DOI: 10.1109/IPEC54454.2022.9777612.
- [30] Li Chen et al. “Full-Duplex SIC Design and Power Allocation for Dual-Functional Radar-Communication Systems”. In: *IEEE Wireless Communications Letters* 12.2 (2023), pp. 252–256. DOI: 10.1109/LWC.2022.3222197.
- [31] Hao Liang and Bin Liao. “Robust Hybrid Beamforming for MIMO-ISAC System with CSI Imperfection”. In: *2023 6th International Conference on Information Communication and Signal Processing (ICICSP)*. 2023, pp. 665–669. DOI: 10.1109/ICICSP59554.2023.10390724.
- [32] Bin Liao, Xue Xiong, and Zhi Quan. “Robust Beamforming Design for Dual-Function Radar-Communication System”. In: *IEEE Transactions on Vehicular Technology* (2023).
- [33] Jing Xu et al. “Sparse Array Design for Joint Communication Radar System via Antenna Selection”. In: *2023 International Symposium on Signals, Circuits and Systems (ISSCS)*. 2023, pp. 1–4. DOI: 10.1109/ISSCS58449.2023.10190916.
- [34] Jing Xu et al. “Sparse Array Design for Joint Communication Radar System via Antenna Selection”. In: *2023 International Symposium on Signals, Circuits and Systems (ISSCS)*. 2023, pp. 1–4. DOI: 10.1109/ISSCS58449.2023.10190916.
- [35] Changhong Yu et al. “Cooperative localisation for multi-RSU vehicular networks based on predictive beamforming”. In: *Annals of Telecommunications* 79.1 (2024), pp. 85–100.